Human prostate epithelium lacks Wee1A-mediated DNA damage-induced checkpoint enforcement

Taija M. Kiviharju-af Hällström*, Sari Jäämaa*, Mia Mönkkönen*, Karita Peltonen*, Leif C. Andersson†‡, René H. Medema§, Donna M. Peehl¶, and Marikki Laiho*‖

*Molecular Cancer Biology Program, Biomedicum Helsinki and Haartman Institute, University of Helsinki, P.O. Box 63, FIN-00014, Helsinki, Finland; †Department of Pathology and Haartman Institute, University of Helsinki Hospital Laboratory Diagnostics, P.O. Box 21, FIN-00014, Helsinki, Finland; ‡Karolinska Institutet, SE 17177, Stockholm, Sweden; §Department of Medical Oncology, Utrecht University Medical Center, 3584 CG, Utrecht, The Netherlands; and ¶Department of Urology, Stanford University School of Medicine, Stanford, CA 94305

Edited by Richard B. Setlow, Brookhaven National Laboratory, Upton, NY, and approved March 8, 2007 (received for review October 20, 2006)

Cellular DNA damage triggers the DNA damage response pathway and leads to enforcement of cell cycle checkpoints, which are essential for the maintenance of genomic integrity and are activated in early stages of tumorigenesis. A special feature of prostate cancer is its high incidence and multifocality. To address the functionality of DNA damage checkpoints in the prostate, we analyzed the responses of human primary prostate epithelial cells (HPECs) and freshly isolated human prostate tissues to γ-irradiation. We find that γ-irradiation activates the ataxia telangiectasia mutated-associated DNA damage response pathway in the HPECs but that the clearance of phosphorylated histone H2AX (γH2AX) foci is delayed. Surprisingly, γ-irradiated HPECs were unable to enforce cell cycle checkpoint arrest and had sustained cyclin-dependent kinase 2 (Cdk2)-associated kinase activity because of a lack of inhibitory Cdk phosphorylation by Wee1A tyrosine kinase. We further show that HPECs express low levels of Wee1A and that ectopic Wee1A efficiently rescues the checkpoints. We recapitulate the absence of checkpoint responses in epithelium of *ex vivo* irradiated human prostate tissue despite robust induction of γH2AX. The findings show that prostate epithelium has a surprising inability to control checkpoint arrest, the lack of which may predispose to accrual of DNA lesions.

p53 | irradiation | cyclin-dependent kinase

The integrity of genomic DNA is challenged by genotoxic insults originating from normal cellular metabolism or from external sources. Cellular responses to DNA damage involve faithful damage surveillance and checkpoint cascades enforcing cell cycle arrest, thus facilitating damage repair, apoptosis, or cellular senescence (1–4). The loss or alterations of genes involved in the damage response pathways almost invariably lead to cancer and have been found both in cancer susceptibility syndromes and in sporadic tumors (4). Furthermore, the DNA damage surveillance pathways are activated during early tumorigenesis presumably because of uncontrolled replicative cycles (5, 6). The acute DNA damage response includes activation of phosphatidyl inositol 3-kinase-related damage sensor and transducer kinases ataxia telangiectasia-mutated (ATM) and ATM and Rad3-related (ATR) phosphorylation of H2AX (γH2AX) and DNA damage foci formation (4, 7). Activated ATM/ATR further propagates the damage signal by phosphorylating and activating checkpoint effector kinases Chk2 and Chk1, leading to proteasome-mediated degradation of phosphatase Cdc25A (3, 8–10). The ATM/ATR–Chk2/Chk1 cascade also functions in the phosphorylation and activation of p53 tumor suppressor protein, resulting in transcriptional induction of $p21^{WAF1/CIP1}$ (hereafter p21) (11). After DNA damage, the cyclin-dependent kinase (Cdk)–cyclin complexes are effectively inhibited by p21 arresting the cells at G_1/S and by down-regulation of Cdc25A maintaining the Wee1A-mediated inhibitory tyrosine 15 (Tyr^{15}) phosphorylation on Cdk1/2, causing an intra-S and G_2/M phase arrest (9, 10). Defects in several of these molecules, including ATM, Chk2, p53, and p21 can lead to an abrogated DNA damage response, including defective cell cycle checkpoints, radioresistant DNA synthesis, and cancer (3, 9, 12).

Prostate cancer is the most common noncutaneous malignancy and the second leading cause of cancer mortality in men. Although extensively investigated, we still have a very rudimentary understanding of the molecular mechanisms leading to the frequent transformation of the prostate epithelium. Furthermore, even though the importance of damage-inducible checkpoint pathways has been recognized as one of the main barriers against tumor formation, research on DNA damage pathways has not been conducted in the prostate. This lack, in part, is the result of few model systems, which include a limited number of established prostate tumor cell lines and mouse models. Prostate tumor cell lines contain numerous genetic changes and are thus unsuitable for studies aiming to elucidate the primary causes for malignant transformation. We therefore took an alternative approach and chose to use primary cultures of human prostatic epithelial cells, derived from radical prostatectomy specimens, as one of our model systems. Four main cell types have been identified in prostatic epithelium: basal cells, transit-amplifying cells, luminal epithelial cells, and neuroendocrine cells. Primary cultures of human prostatic epithelial cells (HPECs), established from prostatectomy specimens, represent prostate progenitor or transit-amplifying cells. These cells are thought to arise from pluripotent stem cells, they express a combination of markers common to both basal and luminal epithelial cells, they have limited self-renewal capacity, and they are in the process of generating differentiated cell populations but are not yet completely committed to a particular lineage (13–15). A growing body of experimental evidence has implicated the proliferating transit-amplifying cells as the cells of origin in prostate cancer (15, 16). Thus, primary cultures of HPECs provide an informative model system for studies into prostate tumorigenesis. In addition, we used a unique model of freshly isolated human prostate tissues obtained from radical prostatectomies to verify our *in vitro* findings.

This report establishes that the primary HPECs and prostatic epithelium have an unexpectedly indulgent checkpoint surveillance, as evidenced by the absence of inhibitory Tyr^{15} phosphorylation on Cdk2, lack of p53 response, radioresistant DNA synthesis, lack of G_1/S and G_2/M phase arrest, and presence of persistent γH2AX

Author contributions: T.M.K.-a.H. and M.L. designed research; T.M.K.-a.H., S.J., M.M., and K.P. performed research; L.C.A., R.H.M., and D.M.P. contributed new reagents/analytic tools; T.M.K.-a.H., S.J., and M.L. analyzed data; and T.M.K.-a.H. and M.L. wrote the paper.

The authors declare no conflict of interest.

This article is a PNAS Direct Submission.

Abbreviations: ATM, ataxia telangiectasia-mutated; ATR, ATM and Rad3-related; Cdk, cyclin-dependent kinase; γH2AX, phosphorylated histone H2AX; HPEC, human prostatic epithelial cell; IR, ionizing radiation.

‖To whom correspondence should be addressed. E-mail: marikki.laiho@helsinki.fi.

This article contains supporting information online at www.pnas.org/cgi/content/full/0609299104/DC1.

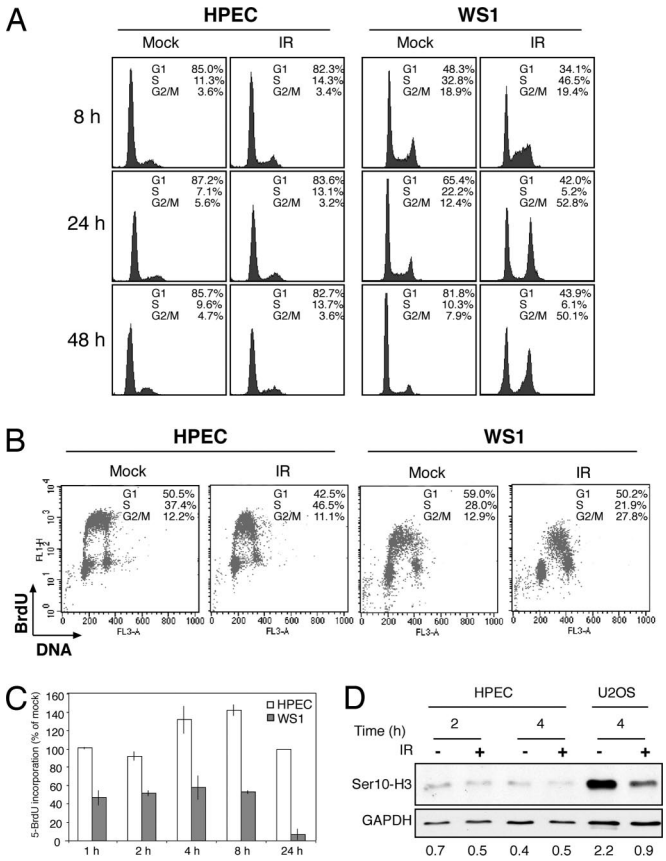

Fig. 1. HPECs lack multiple checkpoints after exposure to DNA damage. (*A*) HPECs and WS1 cells were mock- or IR-treated, and flow cytometric analysis was performed. Results shown are representative of six separate experiments of three HPEC strains. (*B*) HPECs and WS1 cells were mock- or IR-treated, incubated for 4 h, and pulsed with BrdU for the last 30 min. Cells were stained with an anti-BrdU-antibody (*y* axis) and propidium iodide (*x* axis). (*C*) After mock or IR treatment, the cells were labeled with BrdU, and cells positive for BrdU were analyzed by immunofluorescence. Error bars represent SD of duplicate samples. The incorporation of BrdU in IR-treated relative to mock-treated cells is shown. White bars, HPECs; gray bars, WS1 cells. (*D*) Cell extracts were analyzed for the presence of Ser^{10}-phosphorylated histone H3. GAPDH was used as a loading control.

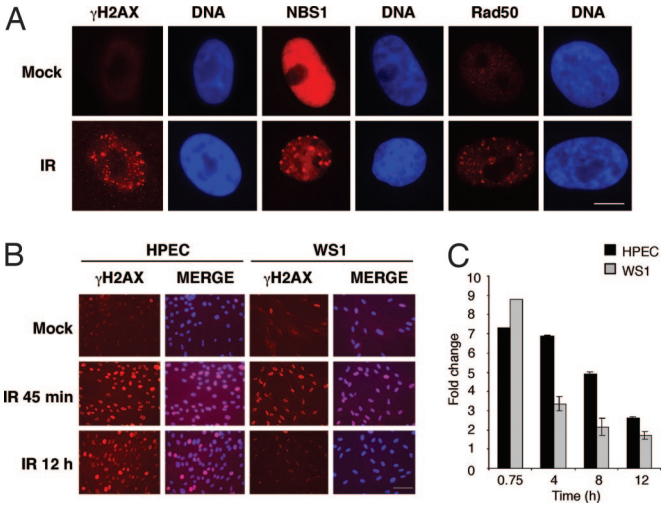

Fig. 2. Sustained DNA damage foci formation in IR-treated HPEC cells. (*A*) HPECs were either mock- or IR-treated (1 Gy), incubated for 45 min, and stained with antibodies against γH2AX, Nbs1, and Rad50 as indicated. Nuclei were stained with Hoechst 33342. (Scale bar, 10 μm.) (*B*) Sustained γH2AX foci in HPECs. HPECs and WS1 cells were either mock- or IR-treated (1 Gy), incubated for the indicated times, and stained for γH2AX. DNA was stained with Hoechst 33342, and the merged images are shown. (Scale bar, 50 μm.) (*C*) Graphical presentation of data in *B*. Fold change in the number of cells positive for γH2AX (>4 foci/cell) is shown. Three hundred cells were analyzed for each time point, and the values represent mean of a duplicate experiment.

damage foci. We ascribe the absence of inhibitory Tyr^{15} phosphorylation to low levels of Wee1A, a tyrosine kinase and negative regulator of cell cycle progression (17–20). Ectopic Wee1A kinase restored Cdk2-Tyr^{15} phosphorylation and efficiently rescued the ionizing radiation (IR)-induced checkpoints in the HPECs. Because variability in the DNA damage responses has been shown to underlie susceptibility to cancer, our results imply that a suboptimal checkpoint arrest may greatly increase the accumulation of genetic lesions in the prostate epithelia.

Results

HPECs Lack Multiple Checkpoints After Exposure to DNA Damage. To investigate the cellular responses of HPECs to IR, we performed flow cytometric analyses and monitored cell cycle distribution at various time points. Checkpoint- proficient IR-treated WS1 human diploid fibroblasts arrested initially in the S phase and subsequently accumulated in the G_2/M phase (Fig. 1*A*). Surprisingly, the cell cycle profiles of IR-treated HPECs were similar to mock-treated cells, indicating a failure to arrest in S or to accumulate in G_2/M after IR (Fig. 1*A*). Similarly, there was no increase in the sub-G_1 fraction of the cells, indicating a lack of apoptosis even at 48 h after IR (Fig. 1*A*). We then pulse-labeled exponentially growing mock- and IR-treated HPECs and WS1 diploid fibroblasts with BrdU and performed multiparameter flow cytometric analyses. A comparison of cell cycle responses indicated that although the WS1 cells presented proper intra-S and G_2/M checkpoint enforcement after IR, there were no corresponding responses in IR-treated HPECs (Fig. 1*B*). We further performed BrdU pulse labeling of the respective cells over an extended period. As expected, the S phase fraction of WS1 cells was reduced by 50% after IR within 1 h, whereas HPECs continued to enter and progress through the S phase even at later time points (Fig. 1*C*). We further tested for the presence of a possible G_2/M phase arrest by using Ser^{10}-phosphorylated histone H3, a mitosis marker. Although in U2OS osteosarcoma cells histone H3 Ser^{10} positivity decreased within 4 h, there was no change in the HPECs, further confirming the absence of G_2/M phase arrest (Fig. 1*D*).

Early DNA Damage Signaling Is Intact in HPECs. To address whether the lack of damage-induced checkpoints was the result of a defect in DNA damage sensor and mediator molecules, we analyzed DNA damage foci formation in IR-treated HPECs. For this purpose, the cells were stained for γH2AX, Nbs1, and Rad50, which are early markers of DNA lesions (2, 7). As shown in Fig. 2*A*, the early damage response was intact, and γH2AX, Nbs1, and Rad50 redistributed into nuclear foci after exposure to IR. To address whether the lack of checkpoint enforcement reflects the rate of recovery from the IR-induced damage, we investigated the number of γH2AX foci-positive HPECs over a time course during which a majority of damage is expected to be repaired (21) and used WS1 cells as a control. In WS1, cells the γH2AX foci were cleared by 12 h (Fig. 2 *B* and *C*). Similar kinetics for clearance was observed in Mv1Lu epithelial cells (data not shown). However, in HPECs the clearance of γH2AX foci was significantly slower, and 36% of IR-treated cells were still positive after 12 h compared with 13% of mock-treated cells (Fig. 2 *B* and *C*). Even at 48 h after treatment, the levels of γH2AX were still elevated by 1.5-fold compared with mock-treated cells (data not shown). These results imply that the

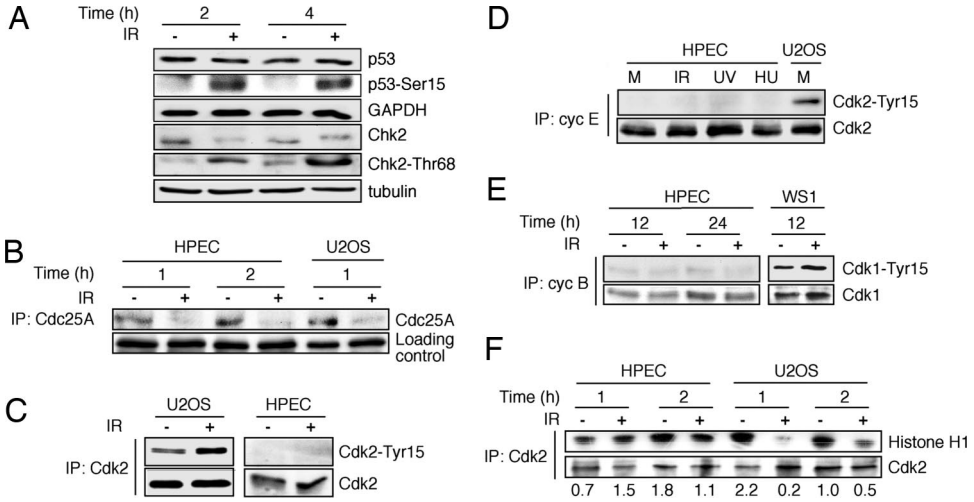

Fig. 3. Sustained Cdk2-associated kinase activity in IR-treated HPECs despite functional ATM-Chk2–Cdc25A–pathway. (*A*) HPECs were either mock- or IR-treated, and the levels of p53, p53-Ser^{15}, Chk2, and Chk2-Thr^{68} were analyzed by Western blotting. GAPDH and β-tubulin were used as loading controls. (*B*) HPECs and U2OS cells were mock- or IR-treated and incubated for the times shown. Cell lysates were precipitated (IP) with an anti-Cdc25A antibody followed by immunoblotting for Cdc25A. (*C*) HPECs and U2OS cells were either mock- or IR-treated, and cellular lysates were precipitated with an anti-Cdk2 antibody followed by immunoblotting analyses for Cdk2-Tyr^{15} and Cdk2. (*D*) Cell lysates from mock-, IR- (10 Gy, 2 h), UVC- (20 J/m^2, 2 h) and hydroxyurea (HU)- (20 mM, 3 h) treated HPECs and control U2OS cells were precipitated with an anti-cyclin E antibody. The levels of cyclin E-bound Cdk2 and Cdk2-Tyr^{15} were evaluated with respective antibodies by Western blotting. (*E*) HPEC and WS1 cells were treated with IR followed by analysis for the levels and Tyr^{15} phosphorylation of cyclin B-associated Cdk1. (*F*) U2OS and HPECs were mock- or IR-treated, and cellular lysates were precipitated with an antibody against Cdk2. Cdk2 was detected by Western blotting, and Cdk2-associated kinase activity was analyzed by using histone H1 as a substrate. Phosphorylation of histone H1 was quantitated and is normalized to total Cdk2 expression.

lack of checkpoint enforcement may lead to persistent damage foci formation in HPECs.

ATM-Directed Kinase Pathway Is Activated, but HPECs Display Sustained Cdk2-Associated Kinase Activity After IR. We then analyzed phosphorylation of ATM downstream targets, Chk2 and p53 (2, 3). Both p53 and Chk2 were phosphorylated on their ATM target residues, Ser^{15} and Thr^{68}, respectively, within 2 h (Fig. 3*A*). However, despite a robust phosphorylation, there was no stabilization of p53, as reported earlier (22). We could detect neither p53 transcriptional activity nor activation of its target gene products p21 and Mdm2 [supporting information (SI) Fig. 6]. As another indicator of a functional ATM–Chk2 cascade, phosphatase Cdc25A was degraded (Fig. 3*B*). These results strongly suggest that the IR-induced ATM-instigated cascade is operational in the HPECs. We next analyzed the status of Cdk2-Tyr^{15} phosphorylation in HPECs and as a comparison, U2OS cells after IR. As reported previously (9), U2OS cells showed robust phosphorylation of Cdk2-Tyr^{15} after IR, whereas this activity was absent in HPECs despite down-regulation of Cdc25A (Fig. 3*C*). To address whether other types of genotoxic insults have the capacity to trigger Cdk2-Tyr^{15} phosphorylation in HPECs, we treated the cells with IR, UVC light, or hydroxyurea and analyzed cell lysates for cyclin E-associated Cdk2-Tyr^{15}. As shown in Fig. 3*D*, there was no detectable Cdk2-Tyr^{15} phosphorylation after any of these treatments in the HPECs, whereas it was easily detectable in mock-treated U2OS cells that had a similar level of cyclin E-associated Cdk2. Similarly, there was no increase in Tyr^{15} phosphorylation of cyclin B-associated Cdk1 (Fig. 3*E*). To relate further the absence of Cdk2-Tyr^{15} phosphorylation in DNA-damaged HPECs to improper checkpoint responses, we analyzed Cdk2 kinase activity in mock- and IR-treated HPEC and U2OS cells. The levels of Cdk2-Tyr^{15} correlated with decreased Cdk2 activity in U2OS cells (9), whereas Cdk2 activity was intact in HPECs after IR (Fig. 3*F*). Taken together, these results indicate that unlike cells with proper DNA damage checkpoints, HPECs fail to induce Cdk2-Tyr^{15} inhibitory phosphorylation, inactivate Cdk2, and delay DNA synthesis in response to damage. Furthermore, the lack of Cdk2-Tyr^{15} inhibitory phosphorylation was a common defect after different types of genotoxic stresses in HPECs.

Ectopic Wee1A Kinase Restores Cdk-Tyr^{15} Phosphorylation and Checkpoint Arrest in Response to IR. Wee1A protein kinase phosphorylates Tyr^{15} of cyclin-associated Cdks and has been implicated in cell cycle transition and checkpoint control (17–20). The level of Wee1A was almost undetectable in HPECs compared with several other cell lines (Fig. 4 *A* and *B*). However, HPECs expressed p63 and p27 abundantly together with keratins specific for both basal and luminal cells, further confirming that the HPECs represent transit-amplifying cells (Fig. 4*B*) (15). To address whether the absence of Wee1A is recapitulated in prostate tissues, we performed immunohistochemical staining for Wee1A and in comparison, for p63 and p27, present in prostate gland basal and luminal cells, respectively (13, 23). Wee1A was coexpressed with p63 in the basal cells but absent in the luminal compartment (Fig. 4*B*). Although Wee1A, based on studies in yeast and cultured cell lines, is considered as a nuclear protein, it was detected both in the nuclear and cytoplasmic compartments of the basal cells.

To test whether the low levels of Wee1A result from the apparent lack of proper p53 responses in HPEC, we treated the cells with Nutlin-3, a p53 activator. However, whereas Nutlin-3a significantly increased p53 levels and led to an arrest of the cells, the Wee1A levels were unaffected, and no Tyr^{15} phosphorylation ensued in response to IR (SI Fig. 7). Furthermore, the IR-induced G_2 checkpoint was completely absent in Nutlin-3 and IR-treated HPECs, and the cells showed complete withdrawal from S phase (SI Fig. 7). Therefore, to address whether the level of Wee1A is rate-limiting for Cdk2-Tyr^{15} phosphorylation, we ectopically expressed Wee1A in HPECs followed by mock or IR treatment. Expression of Wee1A in mock- and IR-treated HPECs induced Cdk2-Tyr^{15} phosphorylation, and this effect was further enhanced by cotransfection of Cdk2 and Wee1A (Fig. 4*C*). Checkpoint-proficient Mv1Lu epithelial cells that were used as a positive control showed a robust increase in Cdk1/2-Tyr^{15} phosphorylation in response to IR, which was further increased in Wee1A-transfected

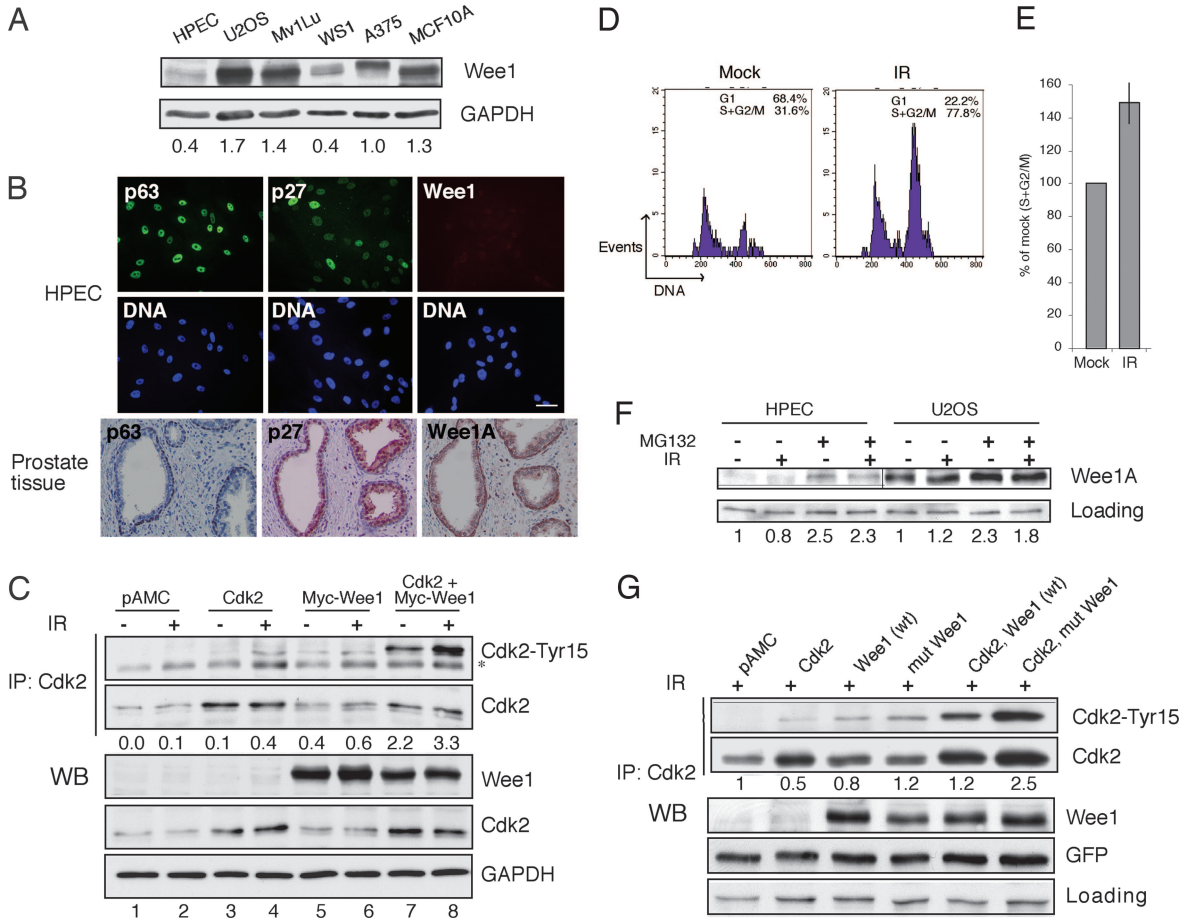

Fig. 4. Ectopic Wee1A kinase restores Cdk-Tyr^{15} phosphorylation and cell cycle checkpoints in response to IR. (*A*) Western blotting analyses of Wee1A levels. (*B*) Expression of Wee1A, p63, and p27 in prostate tissues and in HPECs. Histologically normal sections of prostate tissue or HPECs were stained for the expression of the indicated proteins. (Scale bar, 50 μm.) (*C*) HPECs were transfected either alone or in combination with the expression vectors pAMC, Cdk2, and Myc-Wee1A as indicated and incubated for 48 h. The cells were treated with IR, incubated for 2 h, and total cell lysates were prepared for the analysis of indicated proteins or Tyr^{15}-phosphorylated Cdk2 (asterisk marks a nonspecific band). Cdk2-Tyr^{15} phosphorylation was quantitated and normalized to total Cdk2. Cdk2-Tyr^{15} present in control-transfected cells is set as 0. (*D*) HPECs were transfected with Cdk2 and Myc-Wee1A and were mock- (*Left*) or IR-treated (*Right*) as in *C*. The cells were fixed and stained with a Cdk1/2-Tyr^{15}-specific antibody and subjected to flow cytometry. The cell cycle distribution of Cdk1/2-Tyr^{15}-positive cells is shown. The threshold for Tyr^{15} positivity was set on the basis of signal present in pAMC control-transfected cells. (*E*) The change in the cell cycle distribution of Cdk2-Tyr^{15}-positive cells is indicated as follows: IR(S + G_2/M)/Mock(S + G_2/M). The experiment was performed with three different HPEC strains with similar results. An average of two experiments is shown. (*F*) HPECs and U2OS cells were treated with 10 μM MG132 for 4 h followed by analysis for Wee1A by Western blotting. Normalized Wee1A levels are shown. (*G*) HPECs were transfected either alone or in combination with the following plasmids: control, Cdk2, wild-type Wee1A (wt), and Wee1A phosphodegron mutant (mut; S53A/S123A). GFP was used as a transfection control. Cells were IR-treated and analyzed for Cdk2-Tyr^{15}, Cdk2, and Wee1A. Cdk2-Tyr^{15} phosphorylation was quantitated and normalized to total Cdk2. Cdk2-Tyr^{15} present in control transfected cells is set as 1.

cells (SI Fig. 8). However, ectopic expression of Wee1A did not increase the levels of p53 or produce a p53 IR response (SI Fig. 9).

We then tested whether the cell cycle checkpoints could be restored after ectopic expression of Cdk2 and Wee1A. Mock or IR-treated transiently transfected HPECs were analyzed by flow cytometry for Tyr^{15}-positive cells. Tyr^{15} positivity was detected in cells cotransfected with both Cdk2 and Wee1A, whereas in cells transfected with each vector alone the level of Tyr^{15} was below detection limit (Fig. 4*D* and negative data not shown). After IR, the proportion of Tyr^{15}-positive cells increased in the S and G_2/M phases by 50% compared with mock-treated cells (Fig. 4*E*). These results are in line with a previous report showing that RNAi-mediated down-regulation of Wee1 abolished Tyr^{15} phosphorylation and abrogated the adriamycin-induced G_2 checkpoint in HeLa cells (24).

The low levels of Wee1A (Fig. 4 *A* and *B*) and the related lack of damage-induced Cdk2-Tyr^{15} phosphorylation (Fig. 3*C*) may reflect its inappropriate regulation in HPECs. The exceedingly low levels of Wee1A protein hindered the analyses of the half-life of Wee1A protein in HPECs. Wee1A is down-regulated by protein phosphorylation and consequent degradation by SCF$^{\beta\text{-TrCP}}$ E3-ligase complex (25). Plk1 and Cdk1 phosphorylate Wee1A on Ser^{53} and Ser^{123}, respectively, creating a phosphodegron recognized by β-TrCP (25). Concordant with proteasome mediated degradation of Wee1A, Wee1A was stabilized to a similar extent in HPEC and U2OS cells by treatment with proteasomal inhibitor MG132 (Fig. 4*F*). To address whether the enhanced degradation of Wee1A leads to altered DNA damage responses in HPECs, we transiently transfected HPECs with wild-type (WT) Wee1A, Wee1A phosphodegron mutant (S53A/S123A) alone or in combination with Cdk2, and appropriate transfection controls. After transfection, cells were subjected to IR, precipitated with a Cdk2 antibody, and analyzed for Tyr^{15} phosphorylation. Cdk2-Tyr^{15} phosphorylation in response to IR was more pronounced in cells transfected with the Wee1A mutant (S53A/S123A) than with WT Wee1A and was further increased in cells cotransfected with Cdk2 and Wee1A mutant (S53A/S123A) (Fig. 4*G*). These results indicate that the lack of stress-induced Cdk2-Tyr^{15} inhibitory phosphorylation may be

related to the conditions under which Wee1A kinase is targeted to phosphorylation on Ser^{53} and Ser^{123}. Accordingly, expression of the Wee1A mutant (S53A/S123A) eludes Cdk1-instigated proteasomal turnover and triggers a more robust induction of Cdk2-Tyr^{15} phosphorylation compared with WT Wee1A.

Human Prostate Tissues Lack Cdk1/2-Tyr^{15} and p53 Responses to IR. We then wished to confirm the checkpoint marker protein responses after IR damage in the human prostate. Fresh prostate tissues derived from histologically normal peripheral zone of the prostate were either mock- or IR-treated and stained for Cdk1/2-Tyr^{15}, γH2AX, p53, p21, and p63. There was no increase in Cdk1/2-Tyr^{15} staining in IR-treated tissues, whereas γH2AX staining indicated a robust DNA damage response in the epithelium and in stroma (Fig. 5 and SI Fig. 10*A*). p53 levels were low, and its response to IR remained absent in the irradiated tissues (Fig. 5 and SI Fig. 10*B*). Staining for γH2AX was also evident in a small number of cells localized in areas of basal cell hyperplasia in mock-treated tissues (Fig. 5). Furthermore, there was no increase in p21 staining in IR-treated tissues, although it was detectable in the mock-treated tissue (Fig. 5 and SI Fig. 10*C*). p63 staining was used to mark basal cells and did not undergo any changes after IR (Fig. 5). We cannot fully exclude that the tissue responses are aberrantly regulated after prostatectomy and tissue preparation. However, as another indication that the prostatic tissues maintain viability and capacity to launch appropriate p53 responses, for example, we treated the tissues with a Mdm2 inhibitor Nutlin-3a or nuclear export blocker leptomycin B. In both cases, a robust induction of p53 was detected (SI Fig. 11). These findings strongly suggest that epithelium of fresh human prostate tissue lacks Tyr^{15} and p53 responses in consequence to direct and extensive DNA damage.

Discussion

Using unique human cell and tissue models of the prostate, we provide evidence here that the prostate epithelium has an unexpectedly indulgent checkpoint enforcement. We ascribe this defect to dysregulation of Wee1A tyrosine kinase and p53 (22). The regulation of Wee1A activity and its role in the DNA damage response have been extensively studied in several organisms, but the physiological cues that affect Wee1A levels or localization in mammalian tissues remain unknown. The exceedingly low levels of Wee1A in HPECs, its absence in the luminal epithelial cells, and localization also in the cytoplasmic compartment of the prostate gland basal cells are indicative of its selective regulation in the physiological context. Although increased proteasomal turnover appears to lead to down-regulated Wee1A in HPECs, it does not exclude selective transcriptional repression in the epithelium. Interestingly, down-regulated Wee1A has been identified in a set of genes predicting poor survival in breast, prostate, and lung cancer (26). Furthermore, increased kinase activity of the major Wee1A target, Cdk1, toward androgen receptor leads to increased androgen receptor stability and activity and may thus increase androgen responses in prostate cancer (27). Therefore the control of Wee1A levels may be important not only in the normal epithelium but also in prostate cancer.

Based on the findings here, the ability of Wee1A to phosphorylate Cdk1/2 on Tyr^{15} seems essential in HPECs to instigate a S/G_2 checkpoint arrest, whereas the down-regulation of Cdc25A was insufficient to conserve Tyr^{15}-phosphorylated Cdk2. Therefore, the Tyr^{15} response appears to depend critically on the activity of Wee1A. Hence, the low basal level of Wee1A in transit-amplifying HPECs or in the luminal epithelial cells in the absence of protective repair is likely to predispose these cells to genotoxic stress. Given that Wee1A cytoplasmic translocation has been associated with its inactivation (28) and that Wee1A was observed in the cytoplasm of basal cells, it is possible that the lack of Cdk-Tyr^{15} responses in the prostate basal and luminal cell compartments is caused by absent or inactivated Wee1A. Presently, we find no evidence indicating that the absence of p53 IR responses noted by us and others (22) result from low levels of Wee1A. Conversely, reconstitution of p53 activity in HPECs was without effect on Wee1A nor generated an IR-induced G_2 arrest, indicating that they are uncoupled.

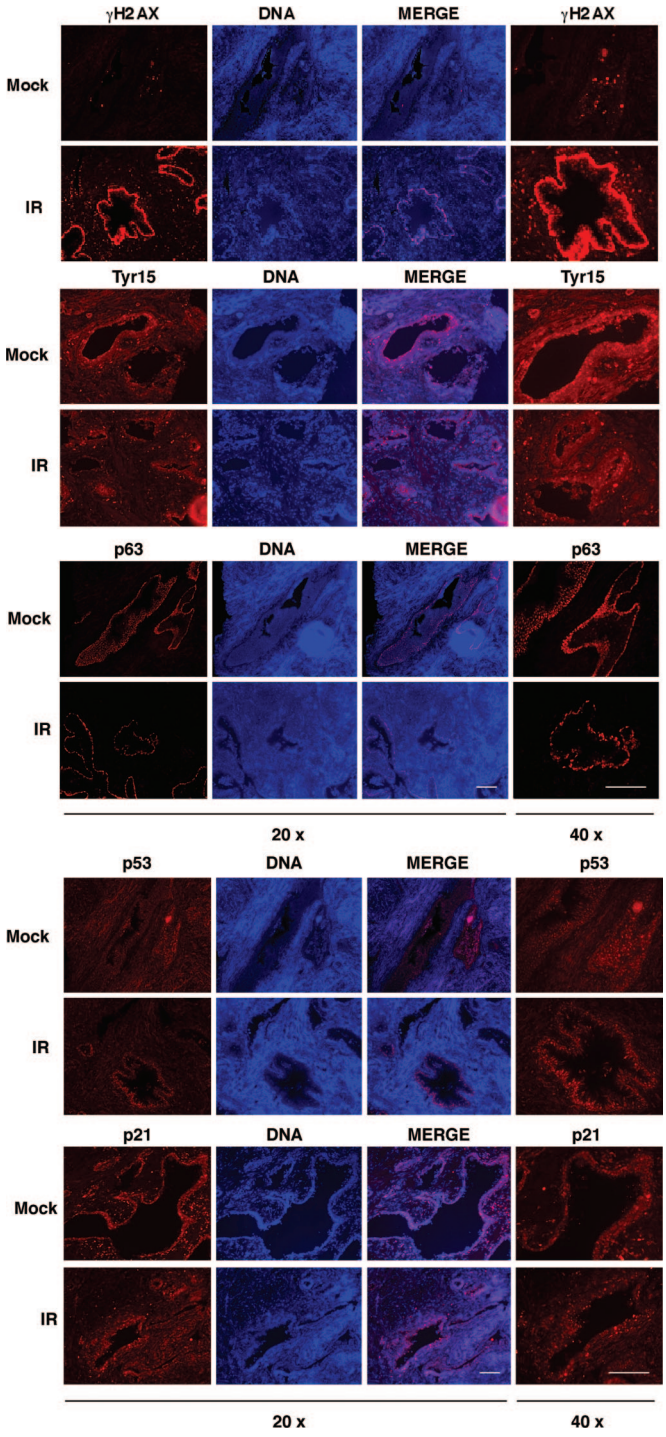

Fig. 5. Human prostatic epithelium lacks Cdk-Tyr^{15} phosphorylation and p53 responses. After prostatectomy, fresh peripheral zone prostate tissue cores were obtained and sliced at 300 μm. Tissue slices were either mock- or IR-treated and incubated for 4 h. Paraffin-embedded sections were stained for Cdk1/2-Tyr^{15}, γH2AX, p53, p21, and p63, and nuclei were counterstained with Hoechst 33342. Images were captured at magnifications of ×20 and ×40 as indicated and represent consecutive sections. (Scale bars, 50 μm.) Images shown are representative of tissues from two prostates.

Unlike cells with intact DNA damage responses, HPECs show aberrations in multiple DNA damage checkpoints after exposure to IR, as reflected by the absence of arrest in G_1 and G_2/M, uninterrupted synthesis of DNA, and lack of apoptosis. It is likely that inadvertent regulation of both Wee1A and p53 contributes to these defects. Furthermore, the slower clearance of DNA damage foci in the presence of continuous replication is suggestive of persistent DNA damage and/or replicative stress. Oxidative stress, for example, through inflammatory processes, has been implicated in the development of prostate cancer and is linked to frequent DNA base lesions concordant with oxidative damage (29). Under these circumstances, cells and tissue environment can be exposed to abnormal amounts of reactive oxygen species produced by inflammatory cells. Because reactive oxygen species are known to induce DNA damage, the surveillance mechanisms to preserve genomic integrity are of extreme importance in an organ such as the prostate, not only challenged by general genotoxic insults but also prone to these organ-specific harmful conditions. The prevalence and multifocal nature of prostate cancer, together with highly frequent DNA structure alterations in normal prostate tissue (29), may result from defective DNA damage checkpoints. In particular, inadequate regulation of cell cycle checkpoints through Wee1A may increase the risk of prostate cancer development.

Materials and Methods

For additional experimental procedures, see *SI Methods*.

Cell Culture and Radiation Treatment. Tissues were dissected from radical prostatectomy specimens. None of the patients had received prior chemical, hormonal, or radiation therapy. HPECs were cultured in MCDB 105 medium (Sigma–Aldrich, St. Louis, MO) with epithelial cell-specific supplements as described previously (30). Six HPEC strains used in this work were derived from histologically normal tissue of the peripheral zone. Experiments were performed with exponentially growing and subconfluent primary cultures. The characteristic traits of primary cultures of human prostatic epithelial cells have been described previously (15). Briefly, HPECs represent prostate progenitor or transit-amplifying cells and express a combination of markers common to both basal (keratin 5, p63) and luminal epithelial cells (keratins 8 and 18), have limited self-renewal capacity, and are in the process of generating differentiated cell populations but have not yet completely committed to a particular lineage. These cells undergo permanent replicative senescence and do not grow in soft agar or form tumors in nude mice. WS1 human skin fibroblasts (CRL-1502) and U2OS osteosarcoma cells (HTB96) were obtained from American Type Culture Collection (Manassas, VA) and cultured according to the supplier's recommendations. Cells were irradiated with 10 Gy, unless otherwise indicated, by using a calibrated ^{137}Cs γ-ray source (BioBeam 8000; STS, Braunschweig, Germany).

***Ex Vivo* Prostate Tissue Cultures.** Tissues were obtained with informed consent and approval of the Stanford Institutional Review Board. Fresh tissue representing histologically normal areas was bored from radical prostatectomy specimens and sliced at 300 μm with a Krumdieck precision tissue slicer (Alabama Research and Development Corporation, Munford, AL). The tissue slices were loaded onto titanium grids in six-well plates containing culture medium and rotated on an inclined plane in a humidified tissue culture incubator at 37°C. The tissue slices were treated with or without IR (10 Gy) and incubated for 4 h. Subsequently, the tissue slices were fixed, embedded in paraffin, and cut at 5 μm. The tissues were then deparaffinized, rehydrated, and the antigens were retrieved in citrate buffer (pH 6.0 and pH 9.9, Antigen Retrieval Solution; DakoCytomation, Carpenteria, CA) by using a microwave oven. The slides were blocked in 5% milk/0.25% Triton X-100/PBS/3% goat nonimmune serum (DakoCytomation) for 30 min. The primary antibodies and dilutions used were as follows: p63, clones 4A4 and Y4A3 (1:100; Lab Vision, Fremont, CA); p53, DO-7 (1:50; DakoCytomation); γH2AX, clone JBW301 (1:800; Upstate Biotechnology, Lake Placid, NY); p21, C-19 (1:1,000; Santa Cruz Biotechnology, Santa Cruz, CA); and Cdk1/2-Tyr^{15} (1:100; Cell Signaling Technology, Beverly, MA, and Calbiochem, San Diego, CA). Alexa 594-conjugated secondary antibodies were from Molecular Probes (Eugene, OR) and the tissues were counterstained with 1 μg/ml Hoechst.

We thank Drs. Scott Lowe and Kari Alitalo for critical reading and comments on the manuscript. We thank Drs. Jiri Lukas, Nobumoto Watanabe, Helen Piwnica-Worms, and William M. Bonner for providing antibodies and expression vectors and Drs. Marcel van Vugt and Randi Syljuåsen for discussions. We thank Maija Hälikkä, Alex Lauderdale, Anni-Helena Sukupolvi, the Molecular Imaging Unit (University of Helsinki), Robert Sellers and Rosey Nolley (Stanford University) for excellent technical assistance. This work was supported by the Academy of Finland (213485), Biocentrum Helsinki, the Finnish Cancer Organizations (to M.L.), the Finnish Cultural Foundation (to T.M.K.-a.H.), and Department of Defense Prostate Cancer Research Program Awards DAMD 17-02-1-0144 and W81XWH-05-1-0111 (to D.M.P.). M.L. is professor of the Foundation for the Finnish Cancer Institute.

1. Hartwell L (1992) *Cell* 71:543–546.
2. Bakkenist CJ, Kastan MB (2004) *Cell* 118:9–17.
3. Bartek J, Lukas C, Lukas J (2004) *Nat Rev Mol Cell Biol* 5:792–804.
4. Kastan MB, Bartek J (2004) *Nature* 432:316–323.
5. Bartkova J, Horejsi Z, Koed K, Kramer A, Tort F, Zieger K, Guldberg P, Sehested M, Nesland JM, Lukas C, *et al*. (2005) *Nature* 434:864–870.
6. Gorgoulis VG, Vassiliou LV, Karakaidos P, Zacharatos P, Kotsinas A, Liloglou T, Venere M, Ditullio RA, Jr, Kastrinakis NG, Levy B, *et al*. (2005) *Nature* 434:907–913.
7. Burma S, Chen BP, Murphy M, Kurimasa A, Chen DJ (2001) *J Biol Chem* 276:42462–42467.
8. Mailand N, Falck J, Lukas C, Syljuasen RG, Welcker M, Bartek J, Lukas J (2000) *Science* 288:1425–1429.
9. Falck J, Mailand N, Syljuasen RG, Bartek J, Lukas J (2001) *Nature* 410:842–847.
10. Sorensen CS, Syljuasen RG, Falck J, Schroeder T, Ronnstrand L, Khanna KK, Zhou BB, Bartek J, Lukas J (2003) *Cancer Cell* 3:247–258.
11. El-Deiry WS, Tokino T, Velculescu VE, Levy DB, Parsons R, Trent JM, Lin D, Mercer WE, Kinzler KW, Vogelstein B (1993) *Cell* 75:817–825.
12. Bunz F, Dutriaux A, Lengauer C, Waldman T, Zhou S, Brown JP, Sedivy JM, Kinzler KW, Vogelstein B (1998) *Science* 282:1497–1501.
13. Garraway LA, Lin D, Signoretti S, Waltregny D, Dilks J, Bhattacharya N, Loda M (2003) *Prostate* 55:206–218.
14. Uzgare AR, Xu Y, Isaacs JT (2004) *J Cell Biochem* 91:196–205.
15. Peehl DM (2005) *Endocr Relat Cancer* 12:19–47.
16. De Marzo AM, DeWeese TL, Platz EA, Meeker AK, Nakayama M, Epstein JI, Isaacs WB, Nelson WG (2004) *J Cell Biochem* 91:459–477.
17. Parker LL, Piwnica-Worms H (1992) *Science* 257:1955–1957.
18. McGowan CH, Russell P (1995) *EMBO J* 14:2166–2175.
19. O'Connell MJ, Raleigh JM, Verkade HM, Nurse P (1997) *EMBO J* 16:545–554.
20. Jin P, Gu Y, Morgan DO (1996) *J Cell Biol* 134:963–970.
21. Rothkamm K, Kruger I, Thompson LH, Lobrich M (2003) *Mol Cell Biol* 23:5706–5715.
22. Girinsky T, Koumenis C, Graeber TG, Peehl DM, Giaccia AJ (1995) *Cancer Res* 55:3726–3731.
23. Signoretti S, Waltregny D, Dilks J, Isaac B, Lin D, Garraway L, Yang A, Montironi R, McKeon F, Loda M (2000) *Am J Pathol* 157:1769–1775.
24. Wang Y, Decker SJ, Sebolt-Leopold J (2004) *Cancer Biol Ther* 3:305–313.
25. Watanabe N, Arai H, Iwasaki J, Shiina M, Ogata K, Hunter T, Osada H (2005) *Proc Natl Acad Sci USA* 102:11663–11668.
26. Liu R, Wang X, Chen GY, Dalerba P, Gurney A, Hoey T, Sherlock G, Lewicki J, Shedden K, Clarke MF (2007) *N Engl J Med* 356:217–226.
27. Chen S, Xu Y, Yuan X, Bubley GJ, Balk SP (2006) *Proc Natl Acad Sci USA* 103:15969–15974.
28. Katayama K, Fujita N, Tsuruo T (2005) *Mol Cell Biol* 25:5725–5737.
29. Malins DC, Johnson PM, Barker EA, Polissar NL, Wheeler TM, Anderson KM (2003) *Proc Natl Acad Sci USA* 100:5401–5406.
30. Peehl DM (1992) in *Culture of Epithelial Cells*, ed Fresney RI (Wiley–Liss, New York), pp 159–180.